UDC 546.3+543.4+539.26 doi: 10.33609/2708-129X.91.11.2025.3-21

STRUCTURE AND SPECTRAL EVALUATION OF COVALENCY IN ND(III) TETRAKIS COMPLEXES WITH CARBACYLAMIDOPHOSPHATE LIGANDS.

Mariia B. Struhatska[a,*], Nataliia S. Kariaka[a], Viktor O. Trush[a], Viktoriya V. Dyakonenko[b], Svitlana V. Shishkina[c], Sergii S. Smola[d], Nataliia V. Rusakova[d], Volodymyr M. Amirkhanov[a]

[a] Faculty of Chemistry, Taras Shevchenko National University of Kyiv, 12 Hetman Pavlo Skoropadsky Str., 01033 Kyiv, Ukraine;
[b] SSI "Institute for Single Crystals", National Academy of Science of Ukraine, 60 Nauky ave., 61072 Kharkiv, Ukraine;
[c] Institute of Organic Chemistry of the National Academy of Sciences of Ukraine, 5 Akademika Kukharya Str., 02660 Kyiv, Ukraine;
[d] A.V. Bogatsky Physicochemical Institute of the National Academy of Sciences of Ukraine, 86 Lustdorfska doroga Str, 65080 Odessa, Ukraine
**e-mail: mariia.struhatska@knu.ua*

Two neodymium(III) tetrakis complexes with different carbacylamidophosphate ligands and a tetraethylammonium cation of the formulas $NEt_4[NdL^1_4]$ (**1Nd**) and $NEt_4[NdL^2_4]\cdot iPrOH$ (**2Nd**) were synthesized, where $[L^1]^-$ is dimethyl-N-trichloroacetylamidophosphate, $Cl_3CC(O)NP(O)(OCH_3)_2^-$, and $[L^2]^-$ is diphenyl-N-trichloroacetylamidophosphate, $Cl_3CC(O)NP(O)(OC_6H_5)_2^-$. The compounds were characterized by elemental analysis, infrared spectroscopy, diffuse reflectance electronic spectroscopy, and single-crystal X-ray diffraction analysis. Structural analysis confirmed the formation of anionic complexes featuring a NdO_8 coordination environment. Coordination polyhedra of central ions are best described as a triangular dodecahedron for **1Nd** and a square antiprism for **2Nd**. Diffuse reflectance spectra in the UV–vis–NIR region revealed characteristic f–f transitions of Nd^{III}, with ligand-dependent modulation of band shape and intensity of the "hypersensitive" transitions. The bonding between the metal and the ligands was found to have weak covalent character. Luminescence studies of the **2Nd** complex revealed weak emission sensitization by the ligands.

Keywords: Nd^{III}, carbacylamidophosphate, tetrakis complex, tetraethylammonium cation, electronic spectroscopy, crystal structure.

INTRODUCTION.

Lanthanide complexes with organic ligands have emerged as key materials in a wide range of high-tech applications, owing to the unique photophysical, magnetic, and catalytic properties imparted by their 4f electronic configuration [1, 2, 3]. Their sharp emission bands, large excitation–emission energy difference, and long excited-state lifetimes make these complexes promising candidates for luminescent devices such as organic light-emitting diodes (OLEDs) [4, 5]. In molecular sensing, lanthanide complexes act as selective probes for detecting molecules, ions, or environmental changes, due to their environment-sensitive emission[6, 7]. In the biomedical field, lanthanides are used in bioimaging and diagnostic agents, where deep tissue penetration and minimal autofluorescence are critical [8, 9]. Other applications of lanthanide(III) complexes with organic ligands include single-molecule magnets [10, 11, 12, 13], structural damage and pressure sensors [14, 15, 16, 17], polymeric optical waveguides and amplifiers [18, 19, 20], security inks [21, 22, 23], luminescent thermometers [24, 25, 26, 27], solar concentrators [28, 29], and catalysis [30, 31].

A structurally appealing subclass of coordination compounds is represented by tetrakis complexes, in which four acido-ligands surround the metal center, typically resulting in discrete anionic units balanced by organic or inorganic counterions [32]. In the case of lanthanides, such tetrakis complexes offer several advantages: high stability, predictable geometry, and elimination of lanthanide luminescence quenching due to saturation of the metal's coordination sites – particularly crucial for NIR-emitting lanthanide ions.

Among the various ligand systems employed for lanthanide complexation [33], carbacylamidophosphates (CAPhs) represent a versatile and promising class. Bidentate CAPh ligands offer phosphoryl and carbonyl oxygen donor atoms, capable of forming air-stable chelates with lanthanide ions. The modular nature of the CAPh framework allows fine-tuning of the photophysical properties of their metal complexes through substitution at the carbon or phosphorus atoms. Moreover, CAPh ligands tend to form rigid complexes with favorable solubility and crystallization behavior and, with suitable substituents and triplet-state energy, they may act as "antennas" and efficiently sensitize Ln^{III} luminescence [32, 34, 35].

Electronic spectroscopy is a valuable tool for characterizing lanthanide complexes, which, unlike transition metal complexes, often display sharp and well-defined electronic transitions due to the shielding of f-electrons within the inner orbitals of the lanthanide ions. Each lanthanide ion exhibits characteristic absorption bands that can provide insight into the coordination environment surrounding the metal ion. Changes in ligand field strength or coordination number may lead to shifts in some of the absorption bands or variations in their intensity [36]. The most commonly studied lanthanide ions in electronic spectroscopy include Pr^{III}, Nd^{III}, Ho^{III}, and Er^{III}, due to the relatively high intensity of their absorption bands [37].

The absorption bands of neodymium(III) in the visible and near-infrared regions arise from intra-4f transitions from the ground state $^4I_{9/2}$, which are Laporte-forbidden but become partially allowed due to mixing of the 4f and 5d orbitals via the ligand field [38]. In Nd^{III} complexes, these bands typically exhibit a ba-

thochromic shift compared to the aqua ion, known as the nephelauxetic shift [39, 40, 41, 42]. The nephelauxetic effect is related to the degree of covalency in the metal-ligand bond within the complex compared to the metal salt in aqueous solution; stronger covalency leads to a larger nephelauxetic shift. The degree of the nephelauxetic shift has been found to depend on the central ion's coordination number [43] and is therefore related to the metal–ligand distance [44]. The polarizability of the ligand also affects the nephelauxetic shift [42]. The multiplicity of the $^2P_{1/2} \leftarrow {}^4I_{9/2}$ transition band, observed around 430 nm, can be used to determine the number of optical centers in a complex and thereby infer the structural individuality of the compound. In the absence of a magnetic field, this transition is degenerate and unaffected by the symmetry field, making its splitting a valuable diagnostic parameter. The so-called "hypersensitive" transition $^4G_{5/2}$, $^2G_{7/2} \leftarrow {}^4I_{9/2}$ near 580–600 nm is responsive to ligand field effects and coordination geometry [45]. Complexation results in a pronounced increase in the intensities of the components of this transition band. The band profile has also been utilized as a diagnostic tool for determining the coordination number of the central metal ion [45, 46], including in complexes with CAPh ligands [47, 48, 53].

In this work, we report the synthesis and comprehensive characterization of two Nd^{III} tetrakis complexes with two types of CAPh ligands, with the formulas $NEt_4[NdL^1_4]$ (**1Nd**) and $NEt_4[NdL^2_4]\cdot iPrOH$ (**2Nd**), where $[L^1]^-$ is deprotonated dimethyl-N-trichloroacetylamidophosphate, $Cl_3CC(O)NP(O)(OCH_3)_2^-$, and $[L^2]^-$ is diphenyl-N-trichloroacetylamidophosphate-anion, $Cl_3CC(O)NP(O)(OC_6H_5)_2^-$. Graphical formulas of the ligands are shown in Figure 1. The compounds were characterized using elemental analysis, single-crystal X-ray diffraction, infrared, and diffuse reflectance electronic spectroscopy. The luminescence properties of the **2Nd** were also studied. The work aims to evaluate how variations in ligand structure influence the coordination geometry, Nd–O bonds covalency, and spectral properties of the Nd^{III} ion in the solid state.

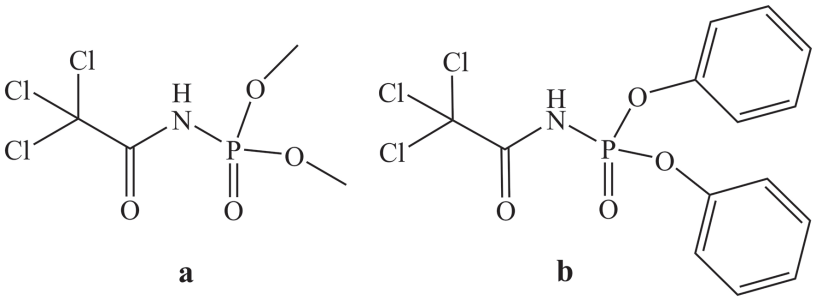

Fig. 1. Graphical formulas of HL^1 (a) and HL^2 (b).

EXPERIMENT AND DISCUSSION OF THE RESULTS.

Materials and methods.

All reagents were obtained from commercial sources and used without further purification. Solvents used in the syntheses were dried using standard literature procedures.

Elemental analysis was performed using a CHNS Vario EL Cube Elemental Analyzer. The lanthanide content in the complexes was

determined by standard titrimetric methods for lanthanide ions [49].

Single-crystal X-ray diffraction data for structure **1Nd** were collected at 294 K using an Xcalibur Sapphire3 diffractometer, and for structure **2Nd** at 296 K using a Bruker APEX-II CCD diffractometer, both equipped with graphite-monochromated MoKa radiation (λ = 0.71073 Å). Using Olex2 software [50], the structures were solved with the SHELXT [51] program using Intrinsic Phasing and refined with the SHELXL [52] refinement package. Full-matrix least-squares refinement against F^2 in anisotropic approximation was used for non-hydrogen atoms. Positions of the hydrogen atoms were located from electron density difference maps and refined by "riding" model with $U_{iso} = nU_{eq}$ of the carrier atom (n = 1.5 for methyl and hydroxyl groups and n = 1.2 for other hydrogen atoms). Crystal data and refinement parameters are summarized in Table 1.

Infrared (IR) spectra were recorded on a Perkin Elmer Spectrum BX spectrometer using KBr pellets in the range of 400–4000 cm^{-1}.

Diffuse reflectance electronic spectra of solid **1Nd** and **2Nd** were measured with a Shimadzu UV-2600i spectrometer.

Emission and excitation spectra of **2Nd** were measured on a "Fluorolog FL 3-22" spectrofluorometer at 298 K.

Synthesis.

The ligands HL^1 and HL^2, as well as their sodium salts, were synthesized according to previously described procedures [34, 53, 54].

The Ln^{III} complexes were obtained according to the following schemes:

$Nd(NO_3)_3 \cdot 6H_2O + 4NaL^1 + NEt_4Cl =$
$= NEt_4[NdL^1_4] + 3NaNO_3 + NaCl + 6H_2O,$

$Nd(NO_3)_3 \cdot 6H_2O + 4NaL^2 + NEt_4Cl + iPrOH =$
$= NEt_4[NdL^2_4] \cdot iPrOH + 3NaNO_3 + NaCl + 6H_2O.$

The hydrated neodymium(III) nitrate (1 mmol, 0.43835 g) was dissolved in acetone (10 mL) under heating for one minute. Next, the dehydrating reagent, triethyl orthoformate (6 mmol, 1 ml), was added, and the resulting solution was boiled for 1 min. Separately, NaL^1 (4 mmol, 1.1696 g) or NaL^2 (4 mmol, 1.6664 g) was dissolved in acetone (10 mL) under heating. Additionally, tetraethylammonium chloride (1 mmol) was dissolved in 2-propanol (5 mL) under heating. The three prepared solutions were combined and refluxed for 10 min. The resulting solution was cooled to room temperature for 10 min, and the precipitated $NaNO_3$ was filtered off. After 1 - 2 days, the target complexes began to crystallize from the filtrate. The compounds were separated from the mother liquor, washed with 2-propanol, and dried in air. The average yields of products **1Nd** and **2Nd** were 55 and 78 %, respectively. The obtained complexes were stable in air, well soluble in methanol, acetone, dimethylformamide (DMF), dimethyl sulfoxide (DMSO), acetonitrile, ethyl acetate, 1,4-dioxane, dichloromethane, chloroform, and in 2-propanol (upon heating). The compounds were insoluble in tetrachloromethane, benzene, hexane, and water.

$NEt_4[NdL^1_4]$ (**1Nd**) Yield: 55 %. M.p.: 157 °C. Anal. Calcd for $C_{24}H_{44}Cl_{12}N_5NdO_{16}P_4$ (M_r = 1352.20) (%): Nd, 10.67; C, 21.32; H, 3.28; N 5.18. Found, %: Nd, 11.3; C, 21.14; H, 3.25; N, 5.32. IR (KBr): ν_{max} = 2992 (w), 2952 (m), 2850 (w), 1620 (vs), 1484 (m), 1462 (w), 1456 (w), 1442 (w, sh), 1393 (w), 1366 (vs), 1186 (s), 1164 (vs), 1046 (vs), 1012 (s), 882 (vs), 845 (s), 836 (s), 820 (s), 780 (m), 726 (m), 674 (m), 548 (s), 498 (m), 460 (m) cm^{-1}.

$NEt_4[NdL^2_4]$·iPrOH (**2Nd**) Yield: 78 %. M.p.: 225 °C. Anal. Calcd for $C_{67}H_{68}Cl_{12}N_5NdO_{17}P_4$ (M_r = 1908.85) (%): Nd, 7.6; C, 42.16; H, 3.59; N 3.67. Found, %: Nd, 8.1; C, 41.67; H, 3.49; N, 3.81. IR (KBr): ν_{max} = 3070 (w), 2924 (m), 2854 (w), 1618 (vs), 1588 (vs), 1490 (vs), 1455 (m), 1440 (w), 1393 (m, sh), 1370 (vs), 1288 (w), 1218 (s), 1192 (vs), 1180 (vs, sh), 1166 (vs), 1072 (w), 1020 (s), 1005 (s, sh), 948 (vs, sh), 939 (vs), 908 (m), 876 (s), 820 (s), 776 (s), 761 (s), 718 (w), 690 (s), 677 (s), 615 (w), 590 (m), 574 (w), 526 (s), 504 (m), 462 (w, sh) cm^{-1}.

X-ray Crystal Structure.

The **1Nd** and **2Nd** complexes crystallize in the monoclinic crystal system in space groups $P2_1/c$ and $C2/c$, respectively. The crystallographic data for the compounds are listed in Table 1. The asymmetric unit cell of **1Nd** and eight of **2Nd** complexes contains one anion $[NdL^1/L^2_4]^-$ ($[L^1]^-$ is a deprotonated dimethyl-N-trichloroacetylamidophosphate, $Cl_3CC(O)NP(O)(OCH_3)_2^-$, and $[L^2]^-$ is diphenyl-N-trichloroacetylamidophosphate-anion, $Cl_3CC(O)NP(O)(OC_6H_5)_2^-$) and one cation NEt_4^+. The **2Nd** complex crystallizes as solvate with isopropanol. Deprotonated CAPh ligands coordinate to the lanthanide ions in a bidentate chelating mode via the oxygen atoms of phosphoryl and carbonyl groups, forming six-membered metallacycles (Figure 2). The coordination polyhedra of the lanthanide ions were determined using the SHAPE 2.1 software [55] as a triangular dodecahedron for **1Nd** and a square antiprism for **2Nd** (Table 2, Figure 3). Compared with the free ligand HL^1 and sodium salt NaL^2 [56], the average bond lengths of P—O and C—O in the **1Nd** and **2Nd** complexes are elongated, while the P—N and C—N bonds are shortened, which is consistent with coordination-induced π-delocalization. The average Ln—O(P) bond lengths are shorter than the Ln—O(C) ones, which is attributed to the stronger affinity of the phosphoryl group for lanthanide ions. However, replacement of substituents from OMe to OPh leads to an elongation of Ln—O(P) bonds and a shortening of Nd—O(C) bonds in **2Nd** compared with **1Nd**. The Nd—O(P) and Nd—O(C) distances vary within 2.374(7)–2.395(8) Å and 2.492(8)–2.499(9) Å, respectively, for complex **1Nd**, and 2.391(7)–2.425(7) Å and 2.432(6)–2.472(7) Å for complex **2Nd**. All the Nd—O bonds are shorter than the sum of the van der Waals radii of oxygen and the Nd^{3+} ionic radius (2.61 Å). The average length of Nd—O bonds in **2Nd** (2.43363 Å) is slightly smaller than in **1Nd** (2.43725 Å). The O—Nd—O bond angles vary from 72.0(3)° to 74.7(3)° for **1Nd** and from 71.6(3)° to 73.5(3)° for **2Nd** (Table 3). The values of the distances and angles are in good agreement with the data obtained for Nd^{III} complexes with CAPhs [57, 58].

As a result of the coordination of Nd atoms by organic ligands in structures **1Nd** and **2Nd**, the six-membered metallacycles are formed. The metallacycles in the **1Nd** and **2Nd** structures are either planar or adopt sofa- or boat-like conformations. The geometric characteristics of the conformations of the six-membered metallacycles are presented in Table 4.

In the crystal phase, the molecules of the anion and cation (in **1Nd**), as well as the anion, cation, and solvent molecules (in **2Nd**), are linked by numerous intermolecular interactions, forming a three-dimensional molecular packing network.

Table 1.

Crystal data and structure refinement parameters for 1Nd and 2Nd.

Parameter	**1Nd**	**2Nd**
formula	$C_{24}H_{44}Cl_{12}N_5NdO_{16}P_4$	$C_{67}H_{48}Cl_{12}N_5NdO_{17}P_4$
M	1352.16	1887.62
T [K]	294	296.15
crystal system	monoclinic	monoclinic
space group	$P2_1/c$	$C2/c$
a [Å]	20.5200(11)	25.610(3)
b [Å]	12.3252(6)	15.281(3)
c [Å]	21.4083(11)	42.846(6)
α [°]	90	90
β [°]	92.577(4)	97.330(13)
γ [°]	90	90
V [Å^3]	5409.0(5)	16631(4)
Z	4	8
Dc [mg cm^{-3}]	1.660	1.509
μ [mm^{-1}]	1.730	1.151
F(000)	2700	7560
crystal size [mm]	0.2 x 0.4 x 0.5	0.1 x 0.2 x 0.3
reflections collected	38576	71669
independent reflections (R_{int})	10616	14544
data/parameters	10616 / 624	14544 / 990
GOF	0.999	1.125
R_1 [I>2σ(I)]	0.098	0.1045
wR_2 [I>2σ(I)]	0.2422	0.1970
R_1 [all data]	0.1698	0.1572
wR_2 [all data]	0.2883	0.2140
CCDC	2486751	2486752

Table 2.

Continuous Shape Measures (CShMs) of the coordination geometry for 1Nd and 2Nd crystal structures.

Label	Symmetry	Shape	**1Nd**	**2Nd**
OP-8	D8h	Octagon	31.986	28.250
HPY-8	C7v	Heptagonal pyramid	23.995	23.297
HBPY-8	D6h	Hexagonal bipyramid	16.557	16.220
CU-8	Oh	Cube	10.324	8.961

Table 2.

Label	Symmetry	Shape	1Nd	2Nd
SAPR-8	**D4d**	**Square antiprism**	1.938	**0.221**
TDD-8	**D2d**	**Triangular dodecahedron**	**0.450**	2.206
JGBF-8	D2d	Johnson gyrobifastigium J26	13.036	16.327
JETBPY-8	D3h	Johnson elongated triangular bipyramid J14	28.648	28.275
JBTPR-8	C2v	Biaugmented trigonal prism J50	2.311	2.934
BTPR-8	C2v	Biaugmented trigonal prism	2.016	2.140
JSD-8	D2d	Snub diphenoid J84	2.205	5.191
TT-8	Td	Triakis tetrahedron	10.878	9.779
ETBPY-8	D3h	Elongated trigonal bipyramid	25.123	23.577

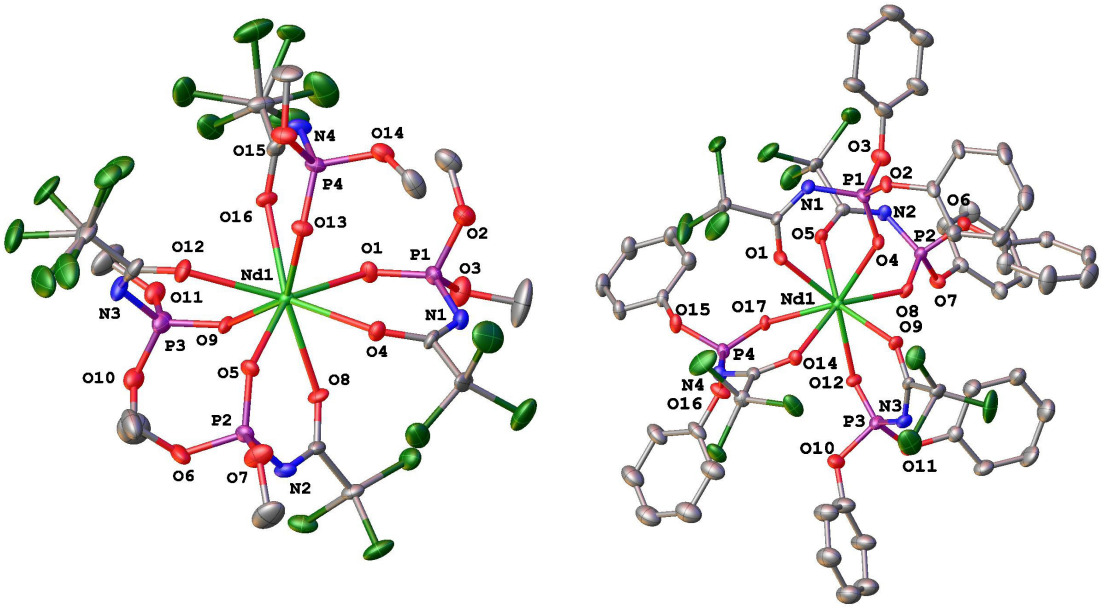

1Nd **2Nd**

Fig. 2. The molecular structures of the $[NdL^1/L^2_4]^-$ anions in 1Nd and 2Nd (H atoms are omitted for clarity). Thermal ellipsoids are shown at 50 % probability level.

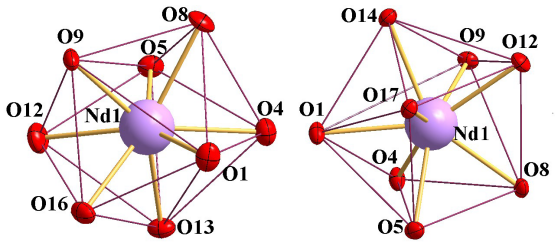

1Nd **2Nd**

Fig. 3. Coordination polyhedra of the Nd^{III} ions in 1Nd and 2Nd.

Table 3.

Selected bond lengths [Å] and angles [°] in 1Nd and 2Nd complexes.

1Nd		**2Nd**	
Nd1—O1	2.395 (8)	Nd1—O1	2.436 (7)
Nd1—O4	2.499 (9)	Nd1—O4	2.391 (7)
Nd1—O5	2.374 (7)	Nd1—O5	2.465 (7)
Nd1—O8	2.482 (7)	Nd1—O8	2.425 (7)
Nd1—O9	2.378 (7)	Nd1—O9	2.472 (7)
Nd1—O12	2.493 (9)	Nd1—O12	2.432 (7)
Nd1—O13	2.385 (7)	Nd1—O14	2.443 (7)
Nd1—O16	2.492 (8)	Nd1—O17	2.405 (6)
P1—O1	1.478 (9)	P1—O4	1.486 (7)
P1—N1	1.589 (13)	P1—N1	1.613 (9)
P2—O5	1.491 (8)	P2—O8	1.482 (7)
P2—N2	1.590 (11)	P2—N2	1.600 (9)
P3—O9	1.479 (8)	P3—O12	1.440 (7)
P3—N3	1.563 (13)	P3—N3	1.608 (10)
P4—O13	1.475 (8)	P4—O17	1.478 (7)
P4—N4	1.564 (11)	P4—N4	1.590 (8)
O4—C3	1.279 (14)	O1—C1	1.227 (11)
O8—C7	1.221 (13)	O5—C15	1.240 (12)
O12—C11	1.27 (2)	O9—C29	1.216 (12)
O16—C15	1.231 (16)	O14—C43	1.273 (12)
N1—C3	1.280 (17)	N1—C1	1.286 (13)
N2—C7	1.355 (16)	N2—C15	1.286 (13)
N3—C11	1.27 (2)	N3—C29	1.298 (14)
N4—C15	1.312 (17)	N4—C43	1.286 (13)
O1—Nd1—O4	72.6 (3)	O1—Nd1—O4	71.6 (2)
O5—Nd1—O8	74.7 (3)	O5—Nd1—O8	71.8 (2)
O9—Nd1—O12	72.7 (3)	O9—Nd1—O12	72.0 (2)
O13—Nd1—O16	73.3 (3)	O14—Nd1—O17	73.5 (2)

Table 4.

The conformational characteristics of six-membered metallocycles in 1Nd and 2Nd.

Cycle	Mean plane atoms, rmsd/Å	Deviation of atom, Å	Type of conformation
1Nd			
Nd1–O1–P1–N1–C3–O4	Nd1…O1…N1…C3 0.01	O4 -0.21(3) P1 -0.21(4)	boat
Nd1–O5–P2–N2–C7–O8	Nd1…O8…C7…N2…O5 0.02	P2 -0.27(4)	sofa
Nd1–O9–P3–N3–C11–O12	Nd1…O9…P3…N3…C11…O12 0.03	–	planar
Nd1–O13–P4–N4–C15–O16	O13…P4…N4…C15…O16 0.03	Nd1 0.45(4)	sofa
2Nd			
Nd1–O4–P1–N1–C1–O1	O4…P1…N1…C1…O1 0.01	Nd1 0.53(4)	sofa
Nd1–O8–P2–N2–C15–O5	Nd1…O8…P2…N2…C15…O5 0.03	–	planar
Nd1–O12–P3–N3–C29–O9	O12…P3…N3…C29…O9 0.02	Nd1 -0.46(5)	sofa
Nd1–O17–P4–N4–C4–O14	Nd1…O17…P4…N4…C4…O14 0.03	–	planar

Infrared spectroscopy

The IR spectra of the **1Nd** and **2Nd** complexes, recorded as KBr pellets in the range of 4000–400 cm^{-1} (Figure 4), confirm the successful coordination of the deprotonated CAPh ligands to the Nd^{III} ions and the presence of tetraethylammonium counterions. The absence of a broad band around 3080 cm^{-1}, which would correspond to the ν(H—N) stretching vibration, indicates that the ligands in the obtained complexes exist in their acidic form. In the high-frequency region, a weak-intensity band at 3070 cm^{-1} corresponds to the C—H stretching vibrations of the phenyl rings in the $(L^2)^-$ ligand of **2Nd**, while medium- and weak-intensity bands in the region 2992–2850 cm^{-1} are assigned to the asymmetric and symmetric C—H stretching vibrations of the methyl groups in $(L^1)^-$ (**1Nd)** and of the methyl and methylene groups in the counterions of both complexes. A strong band at 1620 - 1618 cm^{-1} is assigned to the ν(C=O) stretching vibration of the coordinated carbonyl group. Compared to the free ligands HL^1 [56] and HL^2 [53], this band is shifted to lower wavenumbers in the IR spectra of the complexes, indicating coordination of the C=O group to the Nd^{III} ions through the carbonyl oxygen atom. The aromatic ring skeletal vibrations, involving carbon–carbon stretching, in the spectrum of **2Nd** appear at 1588 and 1490 cm^{-1}. The asymmetric bending vibration $\delta_{as}(CH_3)$ from the NEt_4^+ counterion, as well as from the HL^1 framework, appears at 1455 cm^{-1}, while the symmetric bending vibration $\delta_s(CH_3)$ is observed at 1393 cm^{-1}. The bending vibration $\delta_s(CH_2)$ of the methylene groups is located at 1462 cm^{-1}. Strong bands at 1366 cm^{-1} for **1Nd** and at 1370 cm^{-1} for **2Nd** are attributed to a mixed vibration involving C—C and C—N stretching. The phosphoryl group exhibits several distinct bands: the strong band in the region 1192–1186 cm^{-1} is assigned to the characteristic P=O stretching vibration of the CAPh ligand, while the band at 1166–1164 cm^{-1} corresponds to a coupled P=O and P—N stretching mode. These bands are shifted to lower wavenumbers in the spectra of the synthesized complexes compared to the spectra of the free ligands. Additional band in the region 1046–1020 cm^{-1} represents coupled stretching vibrations ν(PN)*ν(CC) of the ligands. Another strong band at 1012 cm^{-1} in the **1Nd** and at 1020 cm^{-1} in the **2Nd** spectra reflects coupled P=O and P—N stretching vibration. An aromatic C—H in-plane bending band from the ligands in **2Nd** appears at 948 and 1072 cm^{-1}, while the out-of-plane bending is reflected in the bands at 761 and 690 cm^{-1}. The CCl_3 group can be identified by absorption bands of an asymmetric stretching vibration at 780–776 cm^{-1} and a symmetric stretch at 677–674 cm^{-1}. A band at 726–718 cm^{-1} is attributed to chelate ring breathing ν(ϕ). A medium-intensity absorption band that appears in the spectrum of **2Nd** at 590 cm^{-1} is attributed to out-of-plane ring bending. A strong-intensity band at 548 cm^{-1} (**1Nd**) and 526 cm^{-1} (**2Nd)** is assigned to a coupled deformation involving in-plane chelate ring bending and Nd—O stretching modes δ(ϕ)*ν(Nd—O). Medium and weak bands at 504–498 and 462–460 cm^{-1} are assigned to the deformation vibrations of the trichloromethyl group (δ(C-Cl_3)) and in-plane chelate ring bending (δ(ϕ)) of the ligands, respectively. The band assignments were made according to references [59, 60, 61].

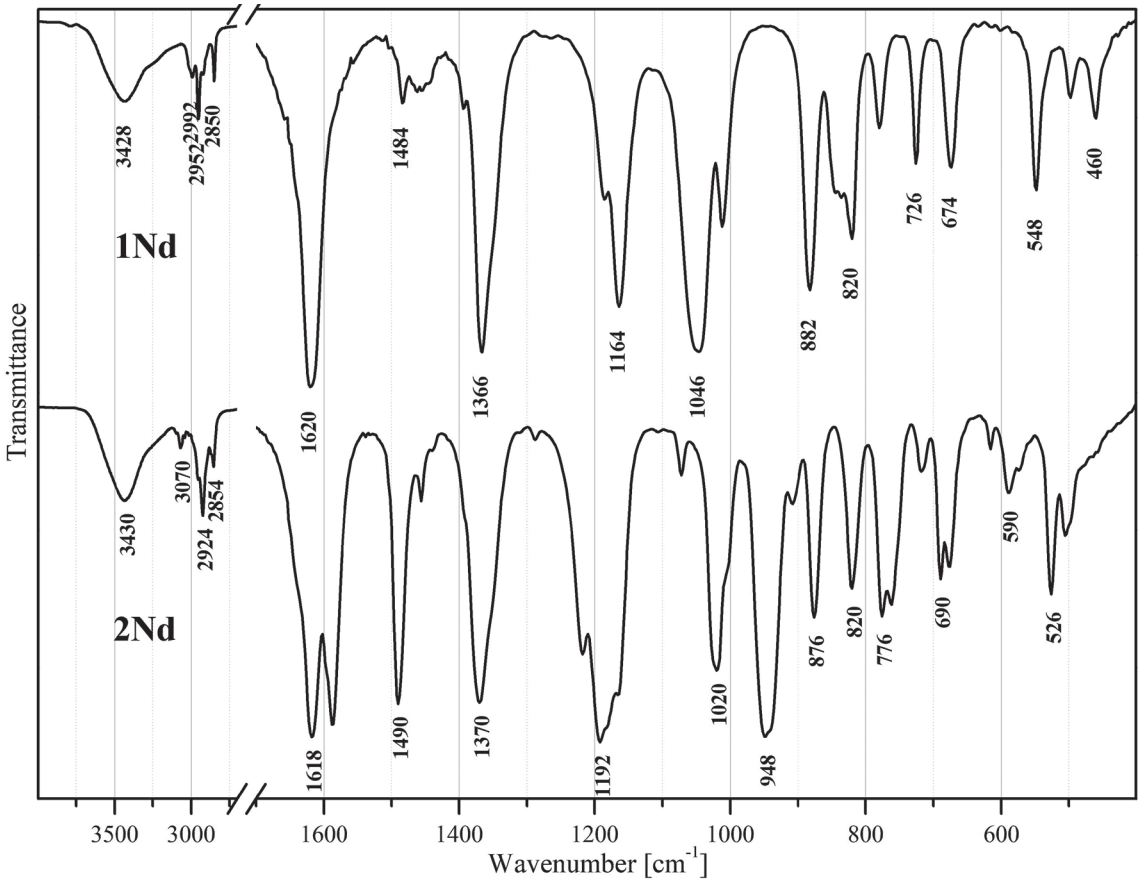

Fig. 4. Mid-FTIR spectra of 1Nd and 2Nd complexes in the form of KBr pellets.

Electronic spectroscopy.

The electronic diffuse reflectance spectra of powders of **1Nd** and **2Nd** complexes were recorded in the 400–900 nm range at room temperature and are shown in Figure 5. Both spectra exhibit characteristic f–f transitions of Nd^{III} ions from the $^4I_{9/2}$ ground state. The absorption bands were assigned according to reference [62]. The hypersensitive transition band in the region near 58–600 nm ($^4G_{5/2}$, $^2G_{7/2} \leftarrow {}^4I_{9/2}$) is similar to that observed in other previously reported CAPh-based lanthanide complexes with a coordination number of eight for the central atom[63, 64, 0]. The relative intensities of the components of this band vary slightly between **1Nd** and **2Nd** due to different coordination polyhedra of the central ions (Table 2). The band of the $^2P_{1/2} \leftarrow {}^4I_{9/2}$ transition, with maxima at 430.4 and 429.2 nm for **1Nd** and **2Nd,** respectively, shows no observable splitting in either spectrum, indicating single crystallographically equivalent Nd^{III} centers in both complexes, consistent with structural data from X-ray diffraction. Electronic transitions from thermally populated higher sublevels of the ground energy level result in the appearance of relatively intense absorption bands in the wavelength range of 432–436 nm.

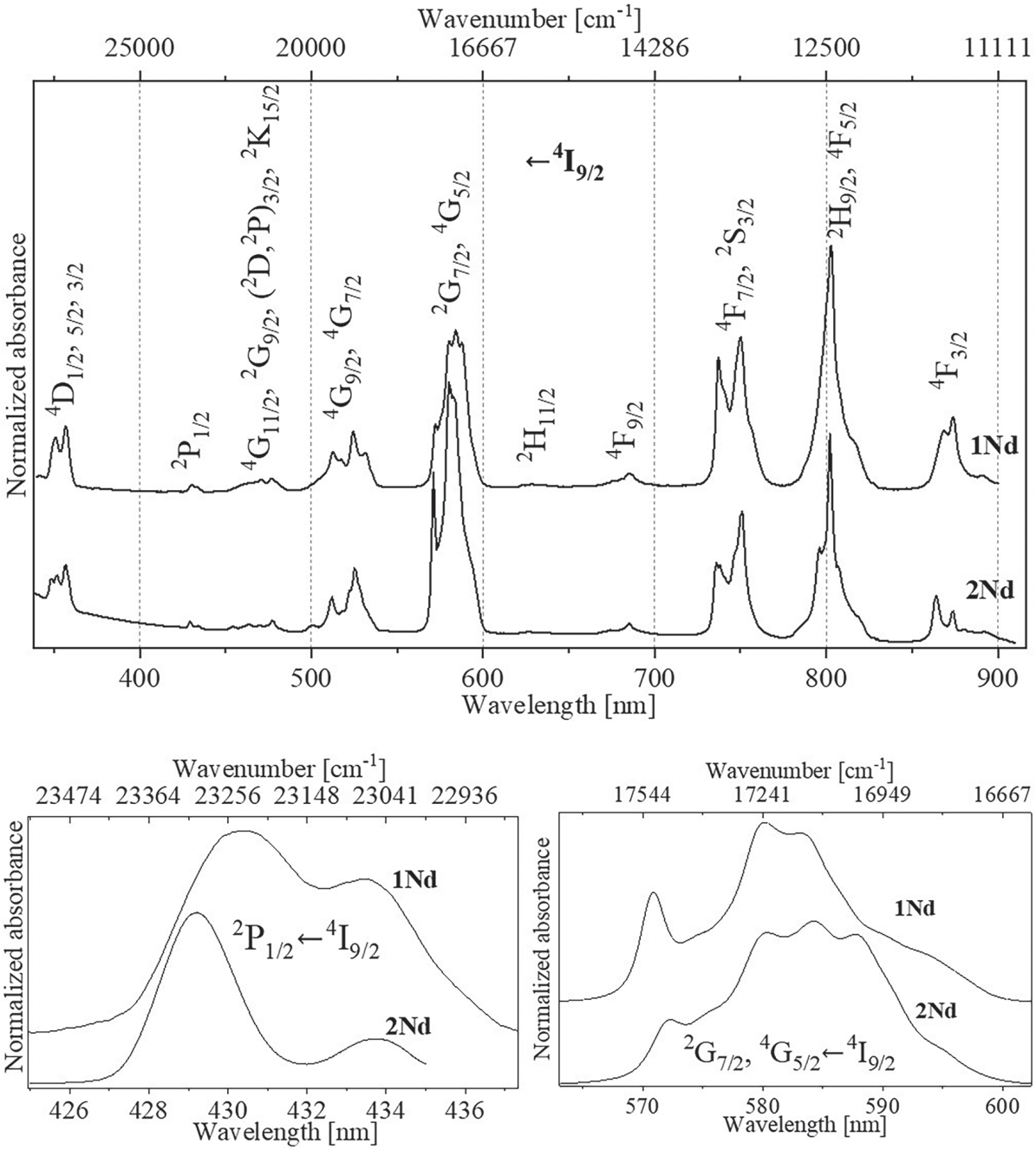

Fig. 5. Electronic diffuse reflection spectra (upper panel); $^2P_{1/2} \leftarrow {}^4I_{9/2}$ and $^2G_{7/2}$, $^4G_{5/2} \leftarrow {}^4I_{9/2}$ transition bands (lower panel) of 1Nd and 2Nd at 300 K.

To evaluate the extent of metal-ligand orbital mixing, the nephelauxetic parameter $\beta = \frac{1}{n}\sum^{n-1} \nu_c^i / \nu_{aq}^i$, the covalency parameter $\delta = \frac{1-\beta}{\beta}100\%$, the bonding parameter $b^{1/2} = \sqrt{\frac{1-\beta}{2}}$ and the angular overlap parameter $\eta = \frac{1-\sqrt{\beta}}{\sqrt{\beta}}$ were calculated by comparing the shifts of the transition bands in the diffuse reflectance spectra of the complexes (ν_c^i) with respect to the positions of the corresponding bands in the spectrum of the Nd^{III} aquo-ion (ν_{aq}^i) (Tables 5, 6) [40, 62, 65]. The obtained results are very similar for the **1Nd** and **2Nd** complexes and suggest weak covalent bonding between the Nd^{III} ions and the ligands, which is in agreement with data reported for other complexes with CAPhs [47]. A slightly larger value of δ for **2Nd** is consistent with the slightly shorter Nd—O bonds in this complex compared to **1Nd**.

Table 5.

Positions of electronic transition spectral band maxima in diffuse reflection spectra of an aquo-ion and 1Nd and 2Nd complexes [cm^{-1}].

J-level	Aquo-ion	**1Nd**	**2Nd**
$^4D_{1/2}$	28850	-	28694
$^4D_{5/2}$	28500	28498	28417
$^4D_{3/2}$	28300	28019	28019
$^2D_{5/2}$	23900	23759	-
$^2P_{1/2}$	23250	23234	23299
$^4G_{11/2}$	21650	21575	21575
$^2G_{9/2}$, $(^2D, ^2P)_{3/2}$	21300	21249	21281
$^2K_{15/2}$	21000	20964	20964
$^4G_{9/2}$	19550	19508	19535
$^4G_{7/2}$	19160	19073	19048
$^2G_{7/2}$	17460	17238	17232
$^4G_{5/2}$	17300	17150	17117
$^2H_{11/2}$	15870	15918	15949
$^4F_{9/2}$	14700	14596	14599
$^4F_{7/2}$, $^2S_{3/2}$	13500	13335	13317
$^2H_{9/2}$	12590	12458	12469
$^4F_{5/2}$	12480	-	12392
$^4F_{3/2}$	11460	11443	11443

Table 6.

The nephelauxetic parameter β, the covalency parameter δ, the bonding parameter $b^{1/2}$ and the angular overlap parameter η for 1Nd and 2Nd.

	β	δ [%]	$b^{1/2}$	η
1Nd	0.99498	0.50471	0.05011	0.00252
2Nd	0.99494	0.50863	0.05030	0.00254

Luminescence spectroscopy

Considering the presence of aromatic substituents in the HL^2, we undertook widespread investigations of **2Nd** for luminescence measurements. The HL^2 ligand possesses a triplet excited state T_1 located at 24270 cm^{-1} [54], which lies significantly above the emissive $^4F_{3/2}$ level of Nd^{3+} (11698 cm^{-1}). The energy gap between the ligand triplet state and the Nd^{III} emitting level is therefore sufficiently large to allow ligand-to-metal energy transfer to occur in **2Nd**. However, the relatively high value of ΔE also implies that additional non-radiative pathways may compete with the sensitization process. In particular, the excess energy gap can facilitate back energy transfer and multiphonon relaxation, which may partially quench the population of the Nd^{III} emissive state. Upon excitation of **2Nd** at 354 nm, the complex exhibits typical f-f emission of the Nd^{III} ion in the NIR region, with narrow bands observed near 900, 1060 and 1330 nm (Figure 6, right panel). The luminescence excitation spectrum of **2Nd**, recorded by monitoring Nd^{III} f-f emission at 1060 nm, exhibits a number of narrow bands, which were assigned to Nd^{III} f-f transitions from the ground $^4I_{9/2}$ level (Figure 6, left panel). The predominance of f-f transitions in the excitation spectrum indicates inefficient sensitization of Nd^{III} emission by the ligands, which is probably due to the large distance between the lanthanide ion and the aromatic substituents in HL^2 as well as due to the excess energy gap between the ligands' lowest triplet state and the emissive level of the neodymium ion, which can facilitate energy dissipation. Earlier, we have reported dimethyl-N-benzoylamidophosphate based complex NEt_4NdL_4 [66], in which, despite of the big energy gap between the ligand triplet state and the Nd^{III} emitting level an efficient sensitization of Nd^{III} emission was observed. This example underlines the importance of the distance between the ligands' chromophore and the lanthanide for efficiency of the antenna effect.

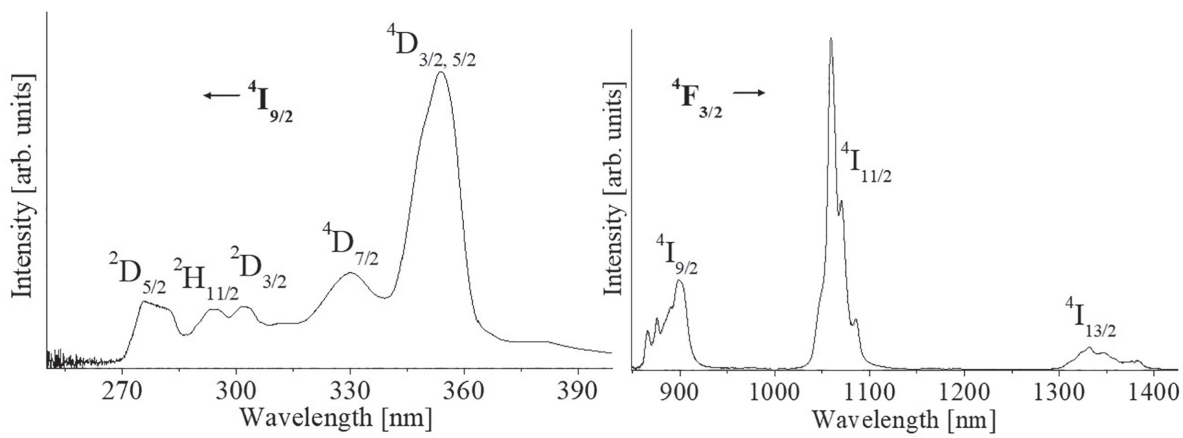

Fig. 6. Luminescence excitation (left panel) and luminescence (right panel) spectra of 2Nd at room temperature.

CONCLUSIONS.

Two new neodymium(III) tetrakis complexes with different carbacylamidophosphate ligands were synthesized and structurally and spectrally characterized.

Structural analysis revealed that variation in the organic substituents on the CAPh ligands results in distinct coordination polyhedra: a triangular dodecahedron in complex **1Nd** and a square antiprism in **2Nd**, both maintaining an eight-coordinate NdO_8 environment. The substitution of OCH_3 with OPh also causes minor differences in metal–ligand distances; however, confirmation of this conclusion requires the investigation of a broader series of related compounds.

Electronic diffuse reflectance spectra of the complexes display well-resolved f–f transitions of Nd^{III}, including hypersensitive bands whose shape depends on the ligand framework. The absence of splitting in the $^2P_{1/2} \leftarrow {}^4I_{9/2}$ transition indicates the presence of a single crystallographically unique Nd^{III} ion in each complex, corroborating the crystallographic data. Covalency parameters (δ, $b^{1/2}$, and η), calculated based on nephelauxetic shifts (β) relative to the Nd^{III} aquo ion, indicate weak covalency in the Nd–ligand bonding. The slightly higher δ value observed for **2Nd** compared to **1Nd** is consistent with shorter metal–ligand distances in the structure of **2Nd**.

Analysis of the excitation spectrum of **2Nd** showed that diphenyl-N-trichloroacetylamidophosphate in this complex insufficiently sensitizes neodymium(III) emission, despite the high enough energy of the ligand triplet state relative to the Nd^{III} emissive level, which highlights the need for future ligand designs that combine appropriate triplet-state alignment with enhanced absorption and improved suppression of nonradiative decay channels.

This study demonstrates that the structural variation in CAPh ligands enables fine-tuning of both coordination geometry and electronic spectral characteristics in lanthanide complexes. These findings support further exploration of CAPh ligands for designing Nd-based materials with tailored spectral properties for potential photonic and sensing applications.

ACKNOWLEDGEMENT. This work was supported by Ministry of Education and Science of Ukraine (grant 22BF037-04).

СТРУКТУРА ТА СПЕКТРАЛЬНА ОЦІНКА КОВАЛЕНТНОСТІ У ТЕТРАКІС-КОМПЛЕКСАХ ND(III) З КАРБАЦИЛАМІДОФОСФАТНИМИ ЛІГАНДАМИ

М. Б. Стругацька[а,*], Н. С. Каряка[а], В. О. Труш[а], В. В. Дьяконенко[б], С. В. Шишкіна[в], С. С. Смола[г], Н. В. Русакова[г], В. М. Амірханов[а]

[а] Хімічний факультет Київського національного університету ім. Тараса Шевченка, вул. Гетьмана Павла Скоропадського, 12, Київ 01033, Україна;

[б] Науково-технологічний комплекс "Інститут монокристалів" Національної академії наук України, просп. Науки, 60, Харків 61072, Україна;

[в] Інститут органічної хімії Національної академії наук України, вул. Академіка Кухаря, 5, Київ 02094, Україна;

[г] Фізико-хімічний інститут ім. О. В. Богатського Національної академії наук України, вул. Люстдорфська дорога, 86, Одеса 65080, Україна

**e-mail: mariia.struhatska@knu.ua*

Синтезовано два тетракіс-комплекси неодиму(III) $NEt_4[NdL^1_4]$ (**1Nd**) та $NEt_4[NdL^2_4]$·iPrOH (**2Nd**) із тетраетиламонієвим катіоном та різними карбациламідофосфатними лігандами: $[L^1]^-$ – диметил-N-трихлорацетиламідофосфат, $Cl_3CC(O)NP(O)(OCH_3)_2^-$, та $[L^2]^-$ – дифеніл-N-трихлорацетиламідофосфат, $Cl_3CC(O)NP(O)(OC_6H_5)_2^-$. Сполуки було охарактеризовано за допомогою елементного аналізу, інфрачервоної спектроскопії, електронної спектроскопії дифузного відбиття та рентгеноструктурного аналізу. Методом РСтА встановлено утворення аніонних комплексів із координаційним оточенням неодиму(III) NdO_8. Координаційні поліедри центральних йонів найкраще описують як трикутний додекаедр у випадку **1Nd** і квадратна антипризма для **2Nd**. Спектри дифузного відбиття в УФ, видимій і ближній ІЧ-області демонструють f–f переходи, характерні для Nd^{III}, при цьому форма та інтенсивність смуг надчутливих переходів залежить від природи лігандів. Було встановлено слабкий ковалентний характер зв'язку метал – ліганд. Дослідження люмінесценції комплексу **2Nd** виявили слабку сенсибілізацію емісії лігандом.

Ключові слова: Nd^{III}, карбациламідофосфат, тетракіс-комплекс, тетраетиламонієвий катіон, електронна спектроскопія, кристалічна структура.

REFERENCES

1. Alexander C., Guo Z., Glover P.B., Faulkner S., Pikramenou Z. Luminescent lanthanides in biorelated applications: from molecules to nanoparticles and diagnostic probes to therapeutics. *Chemical Reviews*. 2025. **125**(4): 2269–2370. https://doi.org/10.1021/acs.chemrev.4c00615
2. Binnemans K. Rare-earth beta-diketonates. *Handbook on the physics and chemistry of rare earths*. Elsevier. 2005. 35: 107–272. https://doi.org/10.1016/S0168-1273(05)35003-3
3. Singh A.K. Multifunctionality of lanthanide-based luminescent hybrid materials. *Coordination Chemistry Reviews*. 2022. **455**: 214365. https://doi.org/10.1016/j.ccr.2021.214365
4. Bünzli J.C.G. Rising stars in science and technology: luminescent lanthanide materials. *European Journal of Inorganic Chemistry*. 2017. **2017**(44): 5058–5063. https://doi.org/10.1002/ejic.201701201
5. de Bettencourt-Dias A. Lanthanide-based emitting materials in light-emitting diodes. *Dalton Transactions*. 2007. **22**: 2229–2241. https://doi.org/10.1039/B702341C
6. Sahoo J., Jaiswar S., Jena H.S., Subramanian P.S. Sensing of phosphate and ATP by lanthanide complexes in aqueous medium and its application on living cells. *Chemistry Select*. 2020. **5**(42): 12878–12884. https://doi.org/10.1002/slct.202002714
7. Bodman S.E., Butler S.J. Advances in anion binding and sensing using luminescent lanthanide complexes. *Chemical Science*. 2021. **12**(8): 2716–2734. https://doi.org/10.1039/D0SC05419D
8. Wang M., Kitagawa Y., Hasegawa Y. Current development of lanthanide complexes for biomedical applications. *Chemistry–An Asian Journal*. 2024. **19**(7): e202400038. https://doi.org/10.1002/asia.202400038
9. Lacerda S., Tóth É. Lanthanide complexes in molecular magnetic resonance imaging and theranostics. *ChemMedChem*. 2017. **12**(12): 883–894. https://doi.org/10.1002/cmdc.201700210
10. Bag P., Rastogi C.K., Biswas S., Sivakumar S., Mereacre V., Chandrasekhar V. Homodinuclear lanthanide {Ln2} (Ln = Gd, Tb, Dy, Eu) complexes prepared from an o-vanillin based

ligand: Luminescence and single-molecule magnetism behavior. *Dalton Transactions*. 2015. **44**(9): 4328–4340. https://doi.org/10.1039/c4dt03429e
11. Gil Y., Aravena D. Understanding Single-Molecule Magnet properties of lanthanide complexes from 4f orbital splitting. *Dalton Transactions*. 2024. **53**(5): 2207–2217. https://doi.org/10.1039/D3DT04179D
12. Wang J., Sun C.Y., Zheng Q., Wang D.Q., Chen Y.T., Ju J.F., Tang Y.F. Lanthanide Single-molecule Magnets: Synthetic strategy, structures, properties and recent advances. *Chemistry–An Asian Journal*. 2023. **18**(7): e202201297. https://doi.org/10.1002/asia.202201297
13. Long J., Guari Y., Ferreira R.A., Carlos L.D., Larionova J. Recent advances in luminescent lanthanide based Single-Molecule Magnets. *Coordination Chemistry Reviews*. 2018. **363**: 57–70. https://doi.org/10.1016/j.ccr.2018.02.019
14. Hirai Y. Triboluminescence of lanthanide coordination polymers. *Assembled lanthanide complexes with advanced photophysical properties*. Singapore: Springer Singapore. 2018. 81–100.
15. Bünzli J.C.G., Wong K.L. Lanthanide mechanoluminescence. *Journal of Rare Earths*. 2018. **36**(1): 1–41. https://doi.org/10.1016/j.jre.2017.09.005
16. Fontenot R.S., Hollerman W.A., Bhat K.N., Aggarwal M.D., Penn B.G. Incorporating strongly triboluminescent europium dibenzoylmethide triethylammonium into simple polymers. *Polymer journal*. 2014. **46**(2): 111–116. https://doi.org/10.1038/pj.2013.78
17. Olawale D.O., Dickens T., Sullivan W.G., Okoli O.I., Sobanjo J.O., Wang B. Progress in triboluminescence-based smart optical sensor system. *Journal of Luminescence*. 2011. **131**(7): 1407–1418. https://doi.org/10.1016/j.jlumin.2011.03.015
18. Moynihan S., Van Deun R., Binnemans K., Redmond G. Optical properties of planar polymer waveguides doped with organo-lanthanide complexes. *Optical Materials*. 2007. **29**(12): 1821–1830. https://doi.org/10.1016/j.optmat.2006.10.005
19. Yang J., Diemeer M.B., Geskus D., Sengo G., Pollnau M., Driessen A. Neodymium-complex-doped photodefined polymer channel waveguide amplifiers. *Optics letters*. 2009. **34**(4): 473–475. https://doi.org/10.1364/ol.34.000473
20. Moynihan S., Van Deun R., Binnemans K., Krueger J., von Papen G., Kewell A., Redmond G. Organo-lanthanide complexes as luminescent dopants in polymer waveguides fabricated by hot embossing. *Optical Materials*. 2007. **29**(12): 1798–1808. https://doi.org/10.1016/j.optmat.2006.10.010
21. Gao M., Li J., Xia D., Jiang L., Peng N., Zhao S., Li G. Lanthanides-based security inks with reversible luminescent switching and self-healing properties for advanced anti-counterfeiting. *Journal of Molecular Liquids*. 2022. **350**: 118559. https://doi.org/10.1016/j.molliq.2022.118559
22. Li J., Xia D., Gao M., Jiang L., Zhao S., Li G. Invisible luminescent inks and luminescent films based on lanthanides for anti-counterfeiting. *Inorganica Chimica Acta*. 2021. **526**: 120541. https://doi.org/10.1016/j.ica.2021.120541
23. Andres J., Hersch R.D., Moser J.E., Chauvin A.S. A new anti-counterfeiting feature relying on invisible luminescent full color images printed with lanthanide-based inks. *Advanced Functional Materials*. 2014. **24**(32): 5029–5036. https://doi.org/10.1002/adfm.201400298
24. Carlotto A., Babetto L., Carlotto S., Miozzi M., Seraglia R., Casarin M., Armelao L. Luminescent thermometers: from a library of europium (III) β-diketonates to a general model for predicting the thermometric behaviour of europium-based coordination systems. *ChemPhotoChem*. 2020. **4**(9): 674–684. https://doi.org/10.1002/cptc.202000116

25. Zhernakov M.A., Sedykh A.E., Denisenko Y.G., Molokeev M.S., Mirzayanov I.I., Becker J., Müller-Buschbaum K. Luminescent thermometer systems Dy3+/Eu3+ and Tb3+/Sm3+ based on coordination compounds: new pairs to the approved Tb3+/Eu3+?. *Chemistry of Materials.* 2024. **36**(19): 9704–9717. https://doi.org/10.1021/acs.chemmater.4c01851
26. Miyata K., Konno Y., Nakanishi T., Kobayashi A., Kato M., Fushimi K., Hasegawa Y. Chameleon luminophore for sensing temperatures: control of metal-to-metal and energy back transfer in lanthanide coordination polymers. *Angewandte Chemie*. 2013. **125**(25). https://doi.org/10.1002/anie.201301448
27. Wang X.D., Wolfbeis O.S., Meier R.J. Luminescent probes and sensors for temperature. *Chemical Society Reviews.* 2013. **42**(19): 7834–7869. https://doi.org/10.1039/c3cs60102a
28. Katsagounos G., Stathatos E., Arabatzis N.B., Keramidas A.D., Lianos P. Enhanced photon harvesting in silicon multicrystalline solar cells by new lanthanide complexes as light concentrators. *Journal of luminescence.* 2011. **131**(8): 1776–1781. https://doi.org/10.1016/j.jlumin.2011.04.023
29. Shahi P.K., Singh P., Rai S.B. Sunlight activated lanthanide complex for luminescent solar collector applications: effect of waveguide matrix. *Journal of Physics D: Applied Physics.* 2017. **50**(7): 075501. https://doi.org/10.1088/1361-6463/aa4ecd
30. Bennett S.D., Core B.A., Blake M.P., Pope S.J., Mountford P., Ward B.D. Chiral lanthanide complexes: coordination chemistry, spectroscopy, and catalysis. *Dalton Transactions* 2014. **43**(15): 5871–5885. https://doi.org/10.1039/C4DT00114A
31. Dicken R.D., Motta A., Marks T.J. Homoleptic lanthanide amide catalysts for organic synthesis: experiment and theory. *Acs Catalysis.* 2021. **11**(5): 2715–2734. https://doi.org/10.1021/acscatal.0c04882
32. Costa I.F., Blois L., Paolini T.B., Assunção I.P., Teotonio E.E., Felinto M.C.F., Brito H.F. Luminescence properties of lanthanide tetrakis complexes as molecular light emitters. *Coordination Chemistry Reviews*. 2024. **502**: 215590. https://doi.org/10.1016/j.ccr.2023.215590
33. Sastri V.R., Perumareddi J.R., Rao V.R., Rayudu G.V.S., Bünzli J.C. Modern aspects of rare earths and their complexes. Amsterdam: Elsevier. 2003. ISBN 0444510109
34. Amirkhanov V., Ovchynnikov V., Trush V., Gawryszewska P., Jerzykiewicz L.B. Powerful new ligand systems: carbacylamidophosphates (CAPh) and sulfonylamidophosphates (SAPh). *Ligands: Synthesis, Characterization and Role in Biotechnology*. New York: NOVA publishers. 2014. 199–248.
35. Kariaka N.S., Lipa A., Carneiro Neto A.N., Malta O.L., Gawryszewska P. and Amirkhanov V.M. Eu3+ and Tb3+ coordination compounds with phenyl-containing carbacylamidophosphates: comparison with selected Ln3+ β-diketonates. *Frontiers in Chemistry*. 2023. **11**: 1188314. https://doi.org/10.3389/fchem.2023.1188314
36. Sinha S.P. Spectroscopic investigations of some neodymium complexes. *Spectrochimica Acta*. 1966. **22**(1): 57–62. https://doi.org/10.1016/0371-1951(66)80008-5
37. Carnall W.T., Fields P.R., Rajnak K. Electronic energy levels in the trivalent lanthanide aquo ions. I. Pr3+, Nd3+, Pm3+, Sm3+, Dy3+, Ho3+, Er3+, and Tm3+. *The Journal of chemical physics*. 1968. **49**(10): 4424–4442. https://doi.org/10.1063/1.1669893
38. Wybourne B.G., Meggers W.F. Spectroscopic properties of rare earths. New York: John Wiley. 1965. 236.
39. Agarwal R.K., Prasad S., Garg R., Sidhu S.K. Synthesis and preliminary structural characterization of some lanthanide (III) semicarbazone complexes. *Bulletin of the Chemical Society of Ethiopia.* 2006. **20**(1): 167–172. http://dx.doi.org/10.4314/bcse.v20i1.21157

40. Sinha S.P. Ternary Lanthanide Complexes of the Type [M(HMPA)4(NO3)3]: A new method of synthesis and spectroscopic studies including a comparison of the electronic spectra of the [M(HMPA)x(ClO4)3] complexes. *Zeitschrift für anorganische und allgemeine Chemie*. 1977. **434**(1): 277–292. https://doi.org/10.1002/zaac.19774340134
41. Wyart J.F., Meftah A., Bachelier A., Sinzelle J., Tchang-Brillet W.Ü.L., Champion N., Sugar J. Energy levels of 4f3 in the Nd3+ free ion from emission spectra. *Journal of Physics B: Atomic, Molecular and Optical Physics*. 2006. **39**(5): L77. http://dx.doi.org/10.1088/0953-4075/39/5/L01
42. Gao F., Zhang S. Investigation of mechanism of nephelauxetic effect. *Journal of Physics and Chemistry of Solids*. 1997. **58**(12): 1991–1994. https://doi.org/10.1016/S0022-3697(96)00139-4
43. Ryan J.L., Jørgensen C.K. Absorption spectra of octahedral lanthanide hexahalides. *The Journal of Physical Chemistry*. 1966. **70**(9): 2845–2857. https://doi.org/10.1021/j100881a021
44. Davidenko N.K., Yatsimirskii K.B. Determination of metal-ligand distances from the position of the spectral bands in lanthanide complexes. *Dokl. Akad. Nauk SSSR*. 1970. **191**(2): 384-387. (in Russian).
45. Karraker D.G. Hypersensitive transitions of six-, seven-, and eight-coordinate neodymium, holmium, and erbium chelates. *Inorganic chemistry*. 1967. **6**(10): 1863–1868. http://dx.doi.org/10.1021/ic50061a018
46. Karraker D.G. Spectral studies on the Nd3+ and Er3+ chelates of heptafluorodimethyloctanedione. *Journal of Inorganic and Nuclear Chemistry*. 1971. **33**(11): 3713–3718. https://doi.org/10.1016/0022-1902(71)80278-6
47. Kariaka N.S., Kolotilov S.V., Gawryszewska P., Kasprzycka E., Weselski M., Dyakonenko V.V., Shishkina S.V., Trush V.A., Amirkhanov V.M. Structures and spectral and magnetic properties of a series of carbacylamidophosphate pentanuclear lanthanide(III) hydroxo complexes. *Inorganic Chemistry*. 2019. **58** (21): 14682–14692. https://doi.org/10.1021/acs.inorgchem.9b02354
48. Pham Y.H., Trush V.A., Korabik M., Amirkhanov V.M., Gawryszewska P. Nd3+ and Yb3+ complexes with N-(diphenylphosphoryl) pyrazine-2-carboxamide as UV-NIR radiation converters and single-ion magnets. *Dyes and Pigments*. 2021. **186**: 108986. http://dx.doi.org/10.1016/j.dyepig.2020.108986
49. Lyle S.J., Rahman M.M. Complexometric titration of yttrium and the lanthanons—I: A comparison of direct methods. *Talanta*. 1963. **10**(11): 1177–1182. https://doi.org/10.1016/0039-9140%2863%2980170-8
50. Dolomanov O.V., Bourhis L.J., Gildea R.J., Howard J.A., Puschmann H. OLEX2: a complete structure solution, refinement and analysis program. *Applied Crystallography*. 2009. **42**(2): 339–341. https://doi.org/10.1107/S0021889808042726
51. Sheldrick G.M. SHELXT – Integrated space-group and crystal-structure determination. *Foundations of Crystallography*. 2015. **71**(1): 3–8. https://doi.org/10.1107/S2053273314026370
52. Sheldrick G.M. Crystal structure refinement with SHELXL. *Crystal Structure Communications*. 2015. **71**(1): 3–8. https://doi.org/10.1107/S2053229614024218
53. Savchuk M.O., Litsis O.O., Sliva T.Yu., Trush V.A., Amirkhanov V.M. Synthesis of diphenyl-N-trichloroacetylamidophosphate and IR spectroscopic investigations of REE anionic coordination compounds on its base. *Voprosy khimii i khimicheskoi tekhnologii*. 2017. **6**: 44–49. ISSN 0321-4095
54. Savchuk M.O., Litsis O.O., Kariaka N.S., Trush V.O., Dyakonenko V.V., Smola S.S., Amirkhanov V.M. Polymeric sodium salts and monomeric lanthanide coordination compounds with diphenyl-N-trichloroacetylami-

dophosphate: synthesis and characterization. *Inorganica Chimica Acta.* 2024. **559**: 121783. https://doi.org/10.1016/j.ica.2023.121783
55. Llunell M., Casanova D., Cirera J., Alemany P., Alvarez S. SHAPE, Ver. 2.0. University of Barcelona: Barcelona, Spain. 2010.
56. Amirkhanov V.M., Trush V.A. Properties and structure of dimethyl ether of trichloroacetylamidophosphoric acid. *Russian Journal of General Chemistry.* 1995. **65**(7): 1120–1124. (in Russian).
57. Kariaka N.S., Dyakonenko V.V., Znovjyak K.O., Shishkina S.V., Amirkhanov V.M. Synthesis, crystal structure and Hirshfeld surface analysis of the tetrakis complex NaNdPyr4(i-PrOH)2·i-PrOH with a carbacylamidophosphate of the amide type. *Structure Reports*. 2023. **79**(12): 1218–1222. https://doi.org/10.1107/S2056989023010071
58. Litsis O.O., Ovchynnikov V.A., Scherbatskii V.P., Nedilko S.G., Sliva T.Y., Dyakonenko V.V., Amirkhanov V.M. Lanthanide mixed-ligand complexes of the [Ln(CAPh)3(Phen)] and [LaxEu1-x(CAPh)3(Phen)] (CAPh= carbacylamidophosphate) type. A comparative study of their spectral properties. *Dalton Transactions.* 2015. **44**(35): 15508–15522. https://doi.org/10.1039/C5DT02557E
59. Sokolnicki J., Legendziewicz J., Amirkhanov W., Ovchinnikov V., Macalik L., Hanuza J. Comparative optical studies of lanthanide complexes with three types of phosphoro-azo derivatives of β-diketones. *Spectrochimica Acta Part A: Molecular and Biomolecular Spectroscopy.* 1999. **55**(2): 349–367. https://doi.org/10.1016/S1386-1425(98)00193-0
60. Coates J. Interpretation of infrared spectra, a practical approach. *Encyclopedia of analytical chemistry.* 2000. **12**: 10815–10837. https://doi.org/10.1002/9780470027318.a5606
61. Silverstein R.M., Webster F.X., Kiemle D.J., Bryce D.L. Spectrometric identification of organic compounds. – 8th ed. Wiley. 2014. 464.
62. Yatsimirskii K.B., Davidenko N.K. Absorption spectra and structure of lanthanide coordination compounds in solution. *Coordination Chemistry Reviews.* 1979. **27**(3): 223–273. https://doi.org/10.1016/S0010-8545(00)82068-8
63. Kariaka N.S., Trush V.A., Medviediev V.V., Dyakonenko V.V., Shishkin O.V., Smola S.S., Amirkhanov V.M. Coordination compounds based on CAPh type ligand: synthesis, structural characteristics and luminescence properties of tetrakis-complexes CsLnL4 with dimethylbenzoylamidophosphate. *Journal of Coordination Chemistry.* 2016. **69**(1): 123–134. http://dx.doi.org/10.1080/00958972.2015.1115024
64. Znovjyak K.O., Moroz O.V., Ovchynnikov V.A., Sliva T.Y., Shishkina S.V., Amirkhanov V.M. Synthesis and investigations of mixed-ligand lanthanide complexes with N,N′-dipyrrolidine-N′′-trichloracetylphosphortriamide, dimethyl-N-trichloracetylamidophosphate, 1,10-phenanthroline and 2,2′-bipyrimidine. *Polyhedron*. 2009. **28**(17): 3731–3738. https://doi.org/10.1016/J.POLY.2009.08.017
65. Henrie D.E., Choppin G.R. Environmental effects on f–f transitions. II. "Hypersensitivity" in some complexes of trivalent neodymium. *The Journal of Chemical Physics.* 1968. **49**(2): 477–481. https://doi.org/10.1063/1.1670099
66. Kariaka N.S., Trush V.A., Dyakonenko V.V., Shishkina S.V., Smola S.S., Rusakova N.V., Sliva T.Y., Gawryszewska P., Carneiro Neto A.N., Malta O.L., Amirkhanov V.M. New luminescent lanthanide tetrakis-complexes NEt4[LnL4] based on dimethyl-N-benzoylamidophosphate. *ChemPhysChem.* 2022. **23**(14): e202200129. https://doi.org/10.1002/cphc.202200129

Стаття надійшла 17.09.2025.